Influences of Brönsted Acidic Sites in H[Al]ZSM-5 on Polarization and Electronegativity of Ethene Studied by Molecular Dynamics

FAN, Jian-Fen[a,b](樊建芬) XIAO, He-Ming*[,b](肖鹤鸣) van de GRAAF, B.[c]
WANG, Qiu-Xia[a](王秋霞) NJO, S. L.[c] XIA, Qi-Ying[a](夏其英)
[a] *Department of Chemistry, Suzhou University, Suzhou, Jiangsu 215006, China*
[b] *Department of Chemistry, Nanjing University of Science and Technology, Nanjing, Jiangsu 210094, China*
[c] *Laboratory of Organic Chemistry and Catalysis, Delft University of Technology, Julianalaan 136, 2628 BL Delft, The Netherlands*

Molecular dynamics simulation has been performed for studying the polarization and electronegativity of ethene molecules near Brönsted acidic sites in H[Al]ZSM-5. The result shows that the molecules are polarized most at the edges of intersections and least at the segments of channels. On the contrary, the highest global molecular electronegativity is found at the centers of channel segments. Al substitution slightly increases the molecular dipole moment, but hardly affects the molecular electronegativity. Brönsted acidic proton decreases the dipole moment of guest molecule, but increases the molecular electronegativity.

Keywords molecular dynamics simulation, ethene, polarization, electronegativity, H[Al]ZSM-5, Brönsted acidic sites

Introduction

Zeolites, microporous aluminosilicalites, an extraordinarily diverse and exciting class of advanced inorganic materials, are known for their catalytic and shape-specific properties concerned with their microporous structures. Adsorption, polarization and subsequent diffusion of guest molecules in zeolite framework are the key points for their applications. It is assumed that polarization is the initial step in many reactions taking place in zeolites. Information about such dynamical properties is difficult to obtain from experimental measurements, and it is useful to complete them with theoretical approaches enabling a good insight into the microscopic processes.

The medium-pore zeolite ZSM-5, first synthesized at MOBIL,[1] has been widely investigated and commercially used. It possesses a bidirectional pore system consisting of two types of intersecting channels. Straight channels are parallel to [010] and sinusoidal channels run along [100]. The resulting intersections are elongated cavities about 0.9 nm in diameter.[2] ZSM-5 only tolerates low levels of aluminum substitutions. The incorporation of an aluminum atom into the structure results in a Brönsted acidic site due to the substitution of a four valence Si atom by a three valence Al atom.

The unique environments of Brönsted acidic protons in zeolite framework significantly affect its overall catalytic behavior. Thermogravimetric adsorption data, IR and NMR spectroscopic data revealed that ethene molecules could be activated on Brönsted acidic sites even at room temperature.[3] Beran[4] carried out semi-empirical quantum chemical calculations to study the interaction between one ethene molecule and the hydroxyl group of HZSM-5 zeolite. The result showed that the interaction led to the formation of a stable π-complex and to the electron transfer from the ethene molecule to the zeolite. Other quantum

* E-mail: xiao@mail.njust.edu.cn
Received March 5, 2001; revised and accepted March 1, 2002.
Project supported by the National Natural Science Foundation of China (No. 29773021) and Education Foundation of Jiangsu Province (No. 98KJB150001).

chemical studies[5,6] showed that ethene molecule interacted with a zeolite proton either in a π-adsorption state or a σ-bonded state. Polarization of guest molecules in the electric field of zeolite framework and other molecules is of interest. Smirnov *et al.*[7] simulated the diffusion of methane in MFI and found that methane molecules were polarized most at the edges of intersections and least at the segments of channels.

Before this work, diffusion of ethene was studied in the lattices of orthorhombic, monoclinic MFI and H[Al]-ZSM-5.[8-10] In this work, our research was focused on how Al and Brönsted acidic proton in the lattice of H[Al]-ZSM-5 affect the polarization and electronegativity of guest ethene molecules. Molecular dynamics (MD) simulation was carried out for the diffusion of 16 ethene molecules in two unit cells of H[Al]ZSM-5 at 300 K. Molecules were treated as totally flexible, while the zeolite framework was supposed to be rigid during the MD run. Analysis of the polarization of guest molecules was based on the consistent implementation[11] of the electronegativity equalization method (EEM) in MD program. EEM developed by Mortier *et al.*[12,13] is a semi-empirical approach to the density function theory, which allows calculations on molecule interaction with infinite crystals, whatever the structure type and chemical position are. Yang *et al.*[14-16] modified the EEM and improved the accuracy in the calculations of atomic charges. It is supposed to be a promising tool for the analysis of zeolite-catalyzed reactions.[17] On the basis of the incorporation of EEM in MD program,[11] the atomic charges depend not only on molecular geometries but also on external potential, *i.e.*, on molecular positions with respect to each other and to zeolite framework. The simulation result shows that molecules are polarized most at the edges of intersections and the highest global molecular electronegativity is found at the centers of channel segments. Brönsted acidic proton decreases the dipole moment of guest molecule, but increases the molecular electronegativity. The trajectory of molecular diffusion reveals that the edges of intersections of the channels in H[Al]ZSM-5 are probably the most active site for reactions.

Method

MD simulation requires a rapidly calculable potential energy function to describe the energy of the system and its first derivative vector as a function of Cartesian coordinates. The latter corresponds to the force acting on an atom in the system. Newton's equations of motion are widely used in MD simulation and are then integrated with the velocity form of the Verlet algorithm.[18] Repetition of this algorithm yields a detailed trajectory of the evolution of a system as a function of time. The accuracy of a simulation as a whole is determined by the length of a time step and the quality of the potential describing the system.[19] Based on EEM,[12,13] the molecular energy at the Born-Oppenheimer surface is written as:

$$E = \sum_i \left([E_i^* + \chi_i^* q_i + \eta_i^* q_i^2] + \frac{1}{2} \sum_{j \neq i} \frac{q_i q_j}{R_{ij}} \right) \quad (1)$$

where q_i is the atomic charge of atom i. The terms enclosed in the square brackets represent the contributions to the intraatomic energy. E_i^*, χ_i^* and η_i^* are expansion coefficients of the intraatomic energy as a function of atomic charge, and the last two coefficients are called electronegativity and hardness of an atom in a molecule, respectively. They are related to the atomic electronegativity and hardness of the free atom.[12] The last term in Eq. (1) describes the interatomic interaction.

For a supermolecular system with M molecules each consisting of N atoms interacting with L atoms of a solid, the potential energy[20] of the molecules can be written as:

$$E = \sum_\alpha^M \sum_i^N \left[(\chi_{i\alpha}^* q_{i\alpha} + \eta_{i\alpha}^* q_{i\alpha}^2) + \frac{1}{2} \sum_\beta^M \sum_{j\beta \neq i\alpha}^N \frac{q_{i\alpha} q_{j\beta}}{R_{i\alpha j\beta}} + \sum_l^L \frac{q_l q_{i\alpha}}{R_{i\alpha l}} \right] + E_{NC} \quad (2)$$

where the index α runs over the molecules, i over the atoms in a molecule, and l over the framework atoms. The first term in the square brackets represents the intraatomic energy, the second and the last stand for the interactions between the molecular atoms and those between molecular and solid atoms, respectively. The last term E_{NC} in Eq.(2) represents all charge-independent terms, including the contributions from bond, angle, torsion, out of plane angle and Lennard-Jones (non-bonded) energies. They can be calculated with appropriate potential functions.[20]

The non-bonded electrostatic and Lennard-Jones interactions in Eq. (2) were truncated at a cut-off distance R_c and shifted-force modification[21] was used for both po-

tentials in order to smooth out the energy and the force to zero at the cut-off distance (R_c). The electrostatic interactions were represented by a shielded potential [$V_{sh}(R)$] shown in Eq. (3).[7] The parameter γ_{ij} was computed as the geometric mean of atomic parameters (γ_i, γ_j).

$$V_{sh}(R) = \frac{q_i q_j}{\left[R^3 + (\frac{1}{\gamma_{ij}})^3\right]^{1/3}} \quad (3)$$

Structural data in MD *simulation*

The initial structure of H[Al]ZSM-5 was created from the optimized monoclinic MFI. Twenty-four crystallographically different T-sites can be distinguished in the lattice of monoclinic MFI.[22] Its optimized structure was obtained by energy minimization with the Delft molecular mechanics (DMM) force field,[20] starting with experimental structure.[2] Theoretical studies[22,23] showed that T2 position was favored for the isomorphouse substitution of Al. In this work, Al substitutions were carried out at four of eight T2 sites in two unit cells of optimized monoclinic MFI, and H additions were each done on different oxygen bridges. The structure was then optimized with the DMM force field to create the optimized H[Al]ZSM-5 with four Brönsted acidic sites in two unit cells. Fig. 1 illustrated its optimized structure. Details can be found in Ref. 24.

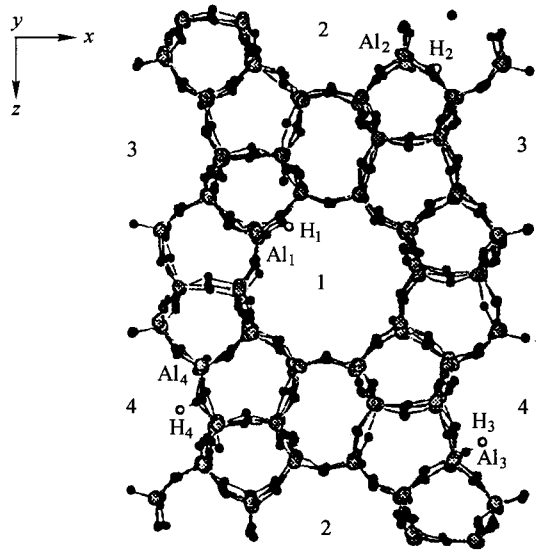

Fig. 1 The optimized structure of H[Al]ZSM-5 with four Brönsted acidic sites. The foot indices indicate the numbering of atoms. The Arabic numbers in the centers of channels represent the numbering of channels.

MD simulation box was defined as two unit cells of the lattice along c axis. The lengths of side x, y and z of the MD simulation box are 2.01391, 1.99162 and 2.67690 nm. Sixteen ethene molecules were uniformly distributed. Details can be found in Ref. 10.

Parameters used in MD *simulation*

In EEM scheme, two parameters (χ^* and η^*) of each atom are needed to compute the atomic charges. The third parameter γ is required due to the introduction of shielded potential to the electrostatic interaction. Table 1 lists the χ^*, η^* and γ parameters which were calibrated to HF/STO-3G atomic charges derived from a Mulliken population analysis. The non-bonded interaction was described as the sum of electrostatic and Lennard-Jones interactions. The Lennard-Jones parameters (σ and ε) were based on Ref. 25. In the present force field, the molecular potential energy is contributed by the bond, angle, torsion, out of plane angle and non-bonded energies. The force field parameters for ethene molecule were chosen from Ref. 20.

Table 1 χ^*, η^* and γ for atoms in simulation box

Atom	Mass	χ^*	η^*	γ
Si	28.08600	3.79552	4.63407	0.21292
O	15.99940	8.50000	7.39796	0.44798
Al	26.98154	0.89502	5.65494	0.20940
H	1.00790	6.41660	6.05239	0.29884
C	12.00000	7.03524	5.35780	0.34225

Simulation procedure

MD simulation was carried out for ethene diffusion in the lattice H[Al]ZSM-5. The simulation box was defined as two unit cells of H[Al]ZSM-5 along c axis. Periodic boundary conditions were applied to simulate the periodicity of the framework. Framework atoms were held fixed at their crystallographic positions, while guest molecules were treated as totally flexible, *i.e.*, all the translational, rotational and vibrational degrees of freedom were taken into account. The cut-off distance was chosen as 0.9 nm for truncating non-bonded electrostatic and Lennard-Jones interactions. The initial velocities of molecular atoms were taken from the Maxwell-Boltzmann distribution at 300 K. The equations of motion were integrated with the velocity form of Verlet algorithm with a time step of

0.5 fs. The first 100000 steps (50 ps) were used for equilibration. The following 755360 steps (377.68 ps) were then performed in NVE ensemble. The data about positions, velocities and charges of atoms were collected every 5th step for the last 655360 steps (327.68 ps), which were carried out in four separate runs (each with 163840 steps). All the calculations were carried out on an Indy workstation at Delft University of Technology, The Netherlands.

Results and discussion

Molecular dipole moment

MD simulation shows that ethene molecules are deformed in the lattice of H[Al]ZSM-5. The maximum and minimum dipole moments for ethene molecules in the lattice of H[Al]ZSM-5 are 0.003 and 1.168 D, respectively. Fig. 2 displays the distribution of molecular dipole moment. Statistical analysis shows that the dipole moments of most molecules are between 0.15 and 0.6 D.

By investigating molecular dipole moments of ethene at different positions in the lattice of H[Al]ZSM-5, it was found that at the centers of segments of straight and sinusoidal channels, molecules are less polarized there, while at the edges of intersections of channels, molecules possess high dipole moments.

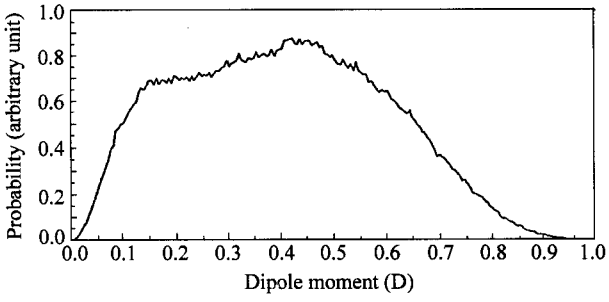

Fig. 2 Distribution of dipole moment of ethene molecules in the lattice of H[Al]ZSM-5.

Further exploring the distributions of molecular dipole moment in the four different straight channels is of interest. In the MD simulation box of H[Al]ZSM-5, there are totally four straight channels. Note that there are one and two Brönsted acidic sites in the straight channel 1 and 4, respectively, but no Brönsted acidic site in the straight channel 3. In the straight channel 2, there is only one Al but no Brönsted acidic proton atom. Table 2 lists the locations of Al and Brönsted acidic proton atoms in the simulation box of H[Al]ZSM-5.

Fig. 3 illustrates how molecular dipole moment depends on the molecular position in the four straight channels of the simulation box. Molecular dipole moment reaches the highest value at the edges of intersections, and the minimum value is found at the centers of the segments. The result shows that the interaction between ethene molecules and the zeolite framework is the strongest at the edges of intersections.

Global molecular electronegativity

Dependence of globe molecular electronegativity on the position in the four straight channels of the simulation box was illustrated in Fig. 3. As compared to the value of 6.42 eV/e of free ethene molecule, the global molecular electronegativity increases in the zeolite. It reaches the highest value of about 8.15 eV/e at the centers of the channel segments, and the lowest value of about 7.7 eV/e is found at the edges of the intersections.

According to Eq. (2), differentiation of molecular potential energy with respect to a Cartesian coordinate u ($u = x, y, z$) of an atom k gives:

$$\frac{\partial E}{\partial u_k} = \sum_{\alpha}^{M}\sum_{i}^{N}\left[\chi_{i\alpha}^{*}\frac{\partial q_{i\alpha}}{\partial u_k} + 2\eta_{i\alpha}^{*}q_{i\alpha}\frac{\partial q_{i\alpha}}{\partial u_k} + \sum_{\beta}^{M}\sum_{j\beta\neq i\alpha}^{N}\frac{q_{j\beta}}{R_{i\alpha j\beta}}\frac{\partial q_{i\alpha}}{\partial u_k} + \sum_{i}^{L}\frac{q_l}{R_{ial}}\frac{\partial q_{i\alpha}}{\partial u_k}\right] - \frac{1}{2}\sum_{\alpha}^{M}\sum_{i}^{N}\sum_{\beta}^{M}\sum_{j\beta\neq i\alpha}^{N}\frac{q_{i\alpha}q_{j\beta}}{R_{i\alpha j\beta}^2}\frac{\partial R_{i\alpha j\beta}}{\partial u_k} - \sum_{\alpha}^{M}\sum_{i}^{N}\sum_{l}^{L}\frac{q_{i\alpha}q_l}{R_{ial}^2}\frac{\partial R_{ial}}{\partial u_k} + \sum_{\alpha}^{M}\sum_{i}^{N}\sum_{l}^{L}\frac{q_{i\alpha}}{R_{ial}}\frac{\partial q_l}{\partial u_k} + \frac{\partial E_{NC}}{\partial u_k} \quad (4)$$

where the terms in square brackets are equal to the electronegativity $\chi_{i\alpha}$ of the atom i in the molecule α and each $\chi_{i\alpha}$ is equal to the global molecular electronegativity χ_α according to the EEM. In the present MD calculations, the charges on atoms of the solid were fixed, that is $\partial q_l/\partial u_k = 0$. With this approximation of constant charge of atoms of the solid, one can obtain:

$$\frac{\partial E}{\partial u_k} = \sum_{\alpha}^{M} \chi_{\alpha}^{ext} \frac{\partial}{\partial u_k} \sum_{i}^{N} \partial q_{i\alpha} - \sum_{\alpha}^{M} \sum_{j \neq k}^{N} \frac{q_{i\alpha} q_k}{R_{ki\alpha}^2} \frac{\partial R_{ki\alpha}}{\partial u_k} - \sum_{l}^{L} \frac{q_k q_l}{R_{kl}^2} \frac{\partial R_{kl}}{\partial u_k} + \frac{\partial E_{NC}}{\partial u_k} \quad (5)$$

The parameter χ_{α}^{ext} is the global electronegativity of the molecule α in the presence of an extramolecular electrostatic potential due to the other molecules and the solid:

$$\chi_{\alpha}^{ext} = \chi_{i\alpha}^{ext} = \left[\chi_{i\alpha}^{*} + 2\eta_{i\alpha}^{*} q_{i\alpha} + \sum_{j\alpha \neq i\alpha}^{N} \frac{q_{j\alpha}}{R_{i\alpha j\alpha}} \right] + \sum_{\beta > \alpha}^{M} \sum_{j\beta}^{N} \frac{q_{j\beta}}{R_{i\alpha j\beta}} + \sum_{l}^{L} \frac{q_l}{R_{i\alpha l}} \quad (6)$$

where the last two terms stand for the external potential from other molecules and solid atoms. It is easily found that the molecular electronegativity is related to the differentiation of molecular potential energy with respect to a Cartesian coordinate.

The difference between dependence of the molecular dipole moment and electronegativity on the molecular position in the straight channels reflects the fact that the former depends on the value of the potential, whereas the latter on the value of the potential gradient. Both depend not only on the molecular geometries but also on the external potential, *i.e.*, on the position of the molecules with the respect to other molecules and to the solid atoms.

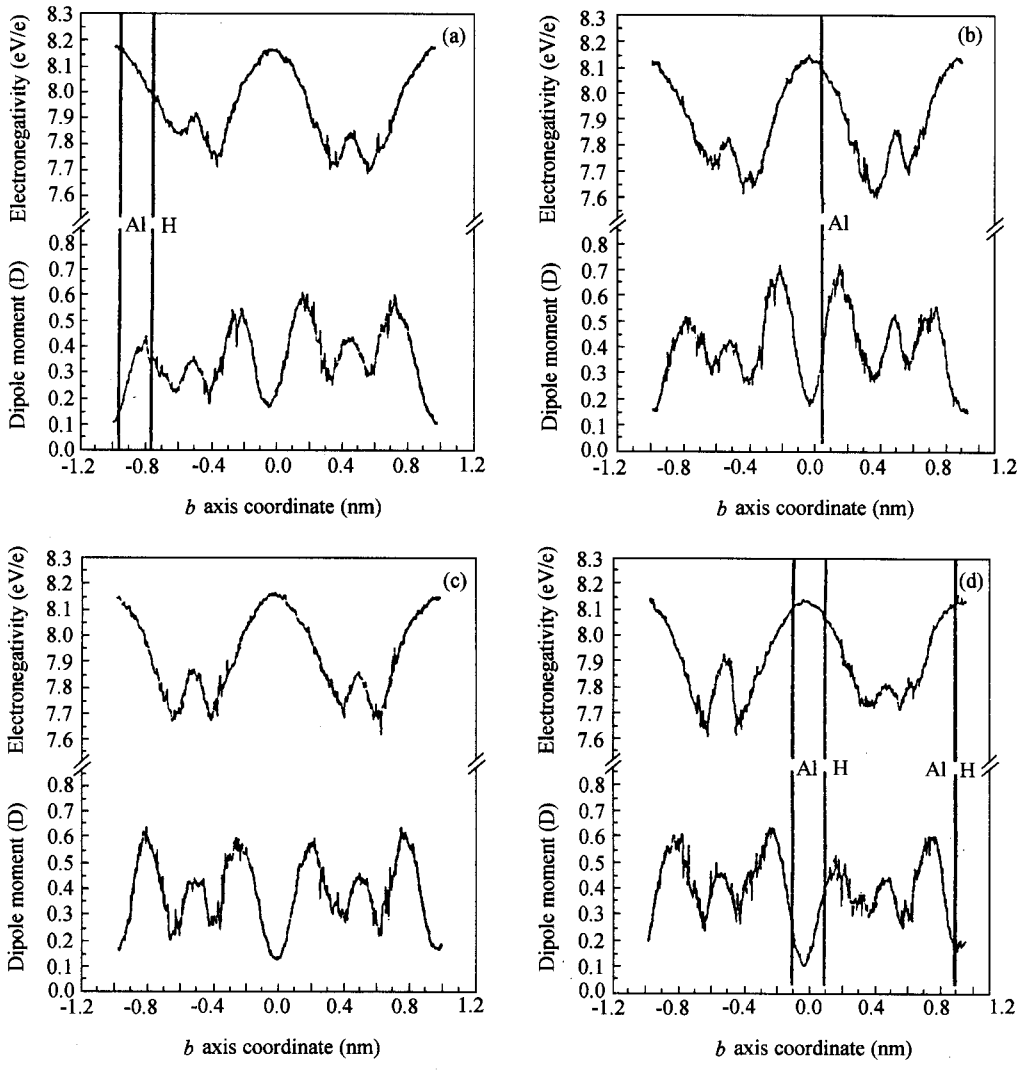

Fig. 3 Dependence of molecular dipole moment and electronegativity on molecular position in the four straight channels of the framework of the simulation box. Intersections are located at ±0.5 nm. (a), (b), (c) and (d) correspond to the results in the straight channel 1, 2, 3 and 4, respectively. The positions of Al and Brönsted acidic H atoms are marked here.

Table 2 Positions of Al and Brönsted acidic proton atoms in two unit cells of H[Al]ZSM-5

Atom[a]	*X*	*Y*	*Z*	Position
Al_1	-3.6388	-9.5382	-1.9442	in the straight channel 1
H_1	-2.0149	-7.5464	-2.6277	in the straight channel 1
Al_2	3.7044	0.3991	-10.8678	in the straight channel 2
H_2	5.3172	2.4405	-10.6623	in a sinusoidal channe l
Al_3	6.4675	-1.1437	8.7880	in the straight channel 4
H_3	7.8278	0.8322	7.9725	in the straight channel 4
Al_4	-6.3564	9.1366	4.4029	in the straight channel 4
H_4	-7.4513	9.1810	6.7499	in the straight channel 4

[a] The foot indices indicate the numbering of atoms. The origin was located at the center of the simulation box.

On the basis of EEM, electronegativity is related to the conception of hardness, which is related to the reactivity of the system. The result shows that molecules possess the highest dipole moment and the lowest electronegativity at the intersection of the channels. This reflects that the intersections are probably the most active sites for reactions.

The difference between Fig. 3(b) and Fig. 3(c) shows that Al substitution slightly increases the molecular dipole moment, but hardly affects the molecular electronegativity. Near an Al site, the molecular dipole moment increases. Comparing Fig. 3(a) and Fig. 3(b) deduces that the molecular dipole moment decreases near a Brönsted acidic proton site whereas the molecular electronegativity there increases. The above phenomena are also manifested in Fig. 3(d).

References

1 Messel, S. L.; McCullough, J. P.; Lechthaler C. H.; Weisz, P. B. *CHEMTECH*. **1976**, *6*, 86.

2 van Koningsveld, H.; Jansen, J. C.; van Bekkum, H. *Zeolites* **1990**, *10*, 235.

3 Bolis, V.; Vedrine, J. C.; van de Berg, J. P.; Wolthuizen, J. P.; Derouane, E. G. *J. Am. Chem. Soc. Faraday Trans*. **1980**, *76*,1606.

4 Beran, S. J. *Mol. Catal*. **1985**, *30*, 95.

5 Kazansky, V. B.; Senchenya, I. N. *J. Catal*. **1989**, *119*, 108.

6 Senchenya, I. N.; Kazansky, V. B. *Catal. Lett*. **1991**, *8*, 317.

7 Smirnov, K. S.; van de Graaf, B. *J. Chem. Soc., Faraday Trans*. **1996**, *92*, 2475.

8 Fan, J.; Xiao, H.; van de Graaf, B.; Njo, S. L. *J. Mol. Sci*. **1998**, *14*, 129.

9 Fan, J.; Xiao, H.; van de Graaf, B.; Njo, S. L. *Chin. Sci. Bull*. **1999**, *44*, 598.

10 Fan, J.; Xia, Q.; Gong, X.; Xiao, H. *Chin. J. Chem*. **2001**, *19*, 251.

11 Smirnov, K. S.; van de Graaf, B. *J. Chem. Soc., Faraday Trans*. **1996**, *92*, 2469.

12 Mortier, W. J.; van Genechten, K.; Gasteiger, J. J. *J. Am. Chem. Soc*. **1985**, *107*, 829.

13 Mortier, W. J.; Ghosh, S. K.; Shankar, S. J. *J. Am. Chem. Soc*. **1986**, *108*, 4315.

14 Yang, Z.; Shen, E. *Sci. China, Ser. B* **1996**, *39*, 20.

15 Yang, Z.; Shen, E. *J. Mol. Struct*. **1996**, *312*, 167.

16 Tang, A.; Yang, Z.; Ye, Y. *Quantum Chemistry of Macromolecular System*, Jilin University Press, Changchun, **2000**.

17 Janssens, G. O. A.; Toufar, H.; Baekelandt B. G.; Mortier, W. J.; Schoonheydt, R. A. *The 11th International Zeolite Conference*, Seoul, **1996**.

18 Swope, W. C.; Anderson, H. C.; Berens, P. H.; Wilson, K. P. *J. Chem. Phys*. **1982**, *76*, 637.

19 Demontis, P.; Suffritti, G. B. In *Modelling of Structure and Reactivity in Zeolites*, Ed.: Catlow, C. R. A., Academic Press Limited, London, **1992**.

20 van Duin, A. C. T.; Bass, J. M. A.; van de Graaf, B. *J. Chem. Soc., Faraday Trans*. **1994**, *90*, 2881.

21 Schrimpf, G.; Schlenkrich, M.; Brickman, J.; Popp, P. *J. Phys. Chem*. **1992**, *96*, 7404.

22 de Vos Burchart, E. *Ph. D. Dissertation*, Delft University of Technology, The Netherlands, **1992**.

23 Derouane, E. G.; Andre, J. M.; Leherte, L.; Galet, P.; Vanderveken, D.; Vercauteren, D. P.; Fripiat, J. G. In *Theoretical Aspects of Heterogeneous Catalysis*, Ed.: Moffat, J. B., van Nostrand Reinhold, New York, **1990**.

24 Fan, J.; Xiao, H.; van de Graaf, B.; Njo, S. L. *Chin. J. Struct. Chem*. **1999**, *18*, 361.

25 Keldsen, G. L.; Nicholas, J. B.; Carrado, K. A.; Winans, R. A. *J. Phys. Chem*. **1994**, *98*, 279.

(E0103055 ZHAO, X. J.; DONG, L. J.)